Engineering Fracture Mechanics
July 2021, Volume 252 Pages 107825 (14p.)
https://doi.org/10.1016/j.engfracmech.2021.107825
https://archimer.ifremer.fr/doc/00700/81173/

Fatigue crack growth properties of carbon-polyamide 6 thermoplastic composites using a multi-ΔG control method

Arhant Mael [1, *], Lolive Eric [2], Bonnemains Thomas [2], Davies Peter [1]

[1] IFREMER, Marine Structures Laboratory, Centre de Bretagne, Plouzané, France
[2] Institut de Recherche Dupuy de Lôme (IRDL - UMR CNRS 6027), Université de Bretagne Occidentale [UBO], France

* Corresponding author : Mael Arhant, email address : mael.arhant@ifremer.fr

Abstract :

The present paper presents a new multi-ΔG control approach to perform mode I fatigue crack growth tests using several constant cyclic energy release rate ranges (ΔG) on only one specimen. It was successfully applied on carbon/polyamide 6 unidirectional composite specimens. After validation checks on the approach, results show that the crack propagation behaviour exhibits three different crack propagation regimes that can be accurately described using the Hartman-Shijves equation. This work has shown that the multi-ΔG control method can provide reliable crack growth propagation results and a complete ΔG versus cycles description.

Highlights

► A new multi-ΔG control approach to perform mode I fatigue crack growth under constant ΔG is presented. ► The crack propagation behaviour can be accurately described using the Hartman-Shijves equation. ► First results concerning the fatigue crack growth behaviour of C/PA6 composites are presented.

Keywords : Thermoplastic composites, Mode I, Fatigue crack growth

1.Introduction

Over the past 50 years, fibre reinforced composite materials have taken over a significant part of the global marketplace in both the aerospace and the marine industries due to their excellent specific properties. For example, the Airbus A350 is now made of more than 50% of composite materials and pleasure boats are almost all made of composite materials. Despite this increasing and growing interest, composites are still special materials to apprehend because of difficulties associated with design (mostly associated with their anisotropic nature) and manufacturing defects. The understanding of the crack growth behaviour, especially under fatigue loads, is a major research subject that has received a lot of interest [1-4]. Nonetheless, there are still open questions concerning the prediction of crack propagation within a composite structure subjected to fatigue cycles. Today, most cyclic crack propagation test methods are based on constant displacements or constant loads, and these do not allow for constant cyclic energy release rates ΔG to be achieved. The early work provided by Ewalds and Wandhill in 1984 [5] described ways to design a constant cyclic stress intensity factor ΔK test by adapting the thickness of the specimen (on metallic specimens). Four years later, in 1988, Russell & Street [6] proposed the first method for composite materials which was able to achieve constant ΔGs. However, the method was not fully automated and measurements of the crack length were made through visual inspection and interrupted tests. Then, in 1995, Tanaka et al. [7] and Hojo and colleagues [8-11] proposed a fully automated ΔG test in which the length of the crack was computed based on compliance measurement. Recently, Manca and colleagues [12] described a new method to run a test on a composite material under an automated and constant ΔG (G_{max}-G_{min}). This is called the G-control method and the reason behind the recent development of the latter is associated with the considerable development in fatigue testing machine controllers in the last few years. Indeed, the G-control method is based on compliance monitoring throughout the test, which implies an algorithm within the method as the crack grows longer, only possible with today's software. Finally, while Manca et al. [12] stated that it is possible to obtain a complete fatigue crack growth plot using only one specimen at different ΔG levels, tests were run at only three ΔG levels in their work. Therefore, it is of particular interest to try and perform a complete fatigue crack growth test while applying a wider range of ΔG levels. Such data would greatly enhance the understanding of crack propagation, and if tests can be performed on one specimen this should also reduce the scatter in data encountered with multi-specimen tests. It may be noted that single specimen tests can be achieved with displacement controlled tests [13], but as of today, not with multi ΔG-control tests. Another aspect that can greatly improve with the G-control method is the test duration. The latter has been discussed several times in the literature, as occupying an expensive test machine for weeks in order to obtain a ΔG versus cycles plot is costly and has resulted in limited published data. Ways to

shorten and optimize cyclic crack tests were described by Brunner et al. in 2009 [14] and Wilk in 2018 [15]. In these studies, replacing the crack length measurement through visual inspection by an automated calculation of the crack length is highlighted as one of the key parameters to optimize the test duration (in addition to frequency optimization). This was originally developed in the mid-80s by Hojo and colleagues [16-18]. This is an essential element in the G-control method.

Most descriptions of fatigue crack growth behaviour are based on the Paris law [19], Eq.1.

$$\frac{da}{dN} = C\Delta G^m \qquad \text{Eq.1}$$

Where $\frac{da}{dN}$ is the crack growth rate in m/cycle, ΔG the cyclic energy release rate in J/m² and C and m are two constants. However, several authors have highlighted limits in the use of the Paris law for composite materials. Martin and Murri [20] showed that in composite materials subjected to mode I fatigue loadings, the value of the exponent m is usually quite high (~5) and this can have a significant effect in design, as any error in load input can lead to large uncertainties in crack propagation. Over the years, several modifications of the Paris law have been suggested. Two interesting reviews of the subject were published in 2013 by Pascoe and colleagues [21] and in 2015 by Khan et al. [22]. Jones et al. [23-25] suggested the use of the Hartman-Shijves equation [26] to describe the fatigue crack growth behaviour in adhesively bonded structures and composites.

Finally, most traditional thermoset matrix composite materials exhibit low interlaminar crack resistance (typically below 1000 J/m² for carbon/epoxy [27]), and delamination is one of the factors limiting more widespread composite use. Thermoplastic matrix composite materials may offer a solution, as some of these materials can provide significantly higher fracture toughness (demonstrated by the development of the use of carbon/PEEK in aviation components). The carbon fibre reinforced polyamide 6 examined here is one such thermoplastic composite, but based on a much cheaper matrix than PEEK. This choice of material was also made due its repairability and recyclability potential. Indeed, thermoplastics are now finding applications in the marine environment [28] due to their more sustainable end-of-life possibilities compared to thermoset composites.

The aim of this paper is to use the G-control method as a means to perform fast and automated fatigue crack growth tests on carbon/polyamide 6 unidirectional composites materials and obtain a complete fatigue crack growth plot using one specimen through a multi-ΔG test. Ultimately, the goal is to validate whether the experimental fatigue crack growth data obtained through the multi ΔG-control method can be represented using the modified Hartman-Shijves equation.

2. Materials and Methods

2.1. Materials

The material used in this study is a continuous fibre reinforced carbon/polyamide 6 unidirectional prepreg from Celanese (Reference: CFR-TP-PA6-CF60-01) with a fibre volume fraction of 48% and a ply thickness of 125 µm. Initial matrix molar mass and crystallinity ratios were respectively measured to be 26.2 kg/mol and 38%. The flexural modulus was taken as 105.6 GPa, from [29], published by the authors on the same material.

2.2. Manufacturing process

Unidirectional composite panels were manufactured by hot compression moulding on a DK Technologies press. Forty composite prepreg plies $[0]_{40}$ were stacked in an aluminium mould designed to manufacture square panels of 280 x 280 x 5 mm^3 (L x l x h). A PTFE film of 25µm thickness was inserted at mid-thickness on one edge of each panel. Insert dimension was 280 x 80 x 0.025 mm^3. The manufacturing cycle used to produce the panels is divided in three steps. First, the mould is heated from ambient temperature up to 240°C at a heating rate of 20°C/min at a pressure slightly below 1 bar. Second, an isothermal stage of 20 minutes at 240°C is used to make sure that all the matrix within the mould is melted. Third, the cooling stage starts. Its rate is the same as the heating rate, i.e. 20°C/min. Moreover, a pressure of 5 bar is applied throughout this last step. It may be noted that if pressure is applied earlier in the cycle, melted matrix flows out of the mould. Finally, such a process allowed us to obtain high quality panels with highly aligned fibres and very low void content (below 1%).

2.3. Double cantilever beam (DCB) tests

2.3.1. Static

Static mode I fracture tests were performed on an Instron 5561 testing machine using a 500 N load cell, at a crosshead speed of 1 mm/min. Crack length was recorded on the specimen edge throughout the tests using a Basler camera at a frame rate of 1 picture per second. Samples were 250 mm long, 20 mm wide and 5 mm thick and were cut using a water jet cutting machine. Three repeat specimens were tested. Glass/Polyamide 6 end blocks with dimensions 20 x 20 x 10 mm^3 were used instead of the more usual aluminium ones as adhesive bonding to thermoplastics is more difficult than to thermosets such as epoxy. With these composite blocks a strong interface was obtained even during fatigue tests. The blocks were bonded using a Loctite 406 adhesive after a Loctite 770 surface treatment. Data analysis was performed according to ASTM 5528 [30] using the compliance calibration (CC) method. This method was chosen because the G-control fatigue test is also based on compliance measurements. All specimens were pre-cracked under mode I loading before test, as the starter film insert was

thicker than that specified by the standard, so only propagation results are shown in this paper. All specimens were dried in dessicators at 0% relative humidity prior to testing.

2.3.2. Fatigue – Multi ΔG control method

G-control fatigue tests were performed on an MTS Acumen 3 Electrodynamic test system at a frequency of 2 Hz and an R-ratio of 0.1 using similar specimens to those presented in 2.3.1 (dimensions and conditioning). The G-control method, described and developed by Manca et al. in [12] was programmed using MTS software (Multipurpose Elite™) to perform the fatigue tests. As stated earlier, this method maintains the cyclic energy release rate ΔG (G_{max}-G_{min}) and R-ratio constant by adjusting the minimum and maximum displacements continuously as the crack grows longer, based on compliance monitoring. The method is clearly explained in [12], however, for clarity it will be summarized here:

As stated earlier, the G-control is based on compliance monitoring C, defined in Eq. 3.

$$C = \frac{\delta}{P} \quad \text{Eq.3}$$

Where δ is the crack opening displacement and P the associated load. The compliance measurement is an essential element of this method, as it allows the calculation of the crack length a, Eq. 4.

$$a = \sqrt[3]{\frac{3EIC}{2}} \quad \text{Eq.4}$$

Where E is the modulus of the specimen in the longitudinal direction and I the moment of inertia of each DCB arm. The R-ratio is classically defined in Eq.5, and can also be expressed in terms of G_{min} and G_{max}, Eq.6.

$$R = \frac{P_{min}}{P_{max}} = \frac{\delta_{min}}{\delta_{max}} \quad \text{Eq.5}$$

$$R_G = \frac{G_{min}}{G_{max}} = R^2 \quad \text{Eq.6}$$

To run a G-control test under displacement control, the cyclic energy release rate ΔG is expressed as follows, Eq. 7:

$$\Delta G = \frac{9EI}{4ba^4}\delta_{max}^2(1 - R^2) \quad \text{Eq.7}$$

Where b is the width of the DBC specimen. Then, to ensure a constant ΔG as the crack grows longer, two requirements must be satisfied, Eq. 8 and Eq. 9.

$$\frac{\delta_{max}}{a^2} = k \quad \text{Eq.8}$$

$$\delta_{min} = R\delta_{max} \quad \text{Eq.9}$$

Where k is a constant. These are the main requirements to perform a G-control test.

In terms of test methodology, one defines the desired ΔG level as well as the R-ratio beforehand in the software. A given number of cycles n is performed. Then, based on compliance measurements, the crack length is calculated and used to determine ΔG. The $\Delta G_{calculated}$ value is then compared to that given to the software initially. If $|\Delta G - \Delta G_{calculated}| > \Delta G_{tolerance}$, the maximum and minimum displacements are adjusted to fit the requirements. If $|\Delta G - \Delta G_{calculated}| < \Delta G_{tolerance}$, the maximum and minimum displacements are kept unchanged. The value of $\Delta G_{tolerance}$ applied here was 10 J/m². These sequences are then repeated within a loop for a given number of cycles N. Such a loop allows the determination of the crack growth rate at the desired ΔG level.

One very interesting feature of the method is that it is possible to use only one specimen and obtain a complete fatigue curve da/dN=f(ΔG) if the test is performed at different ΔG levels. To do so, the loop previously described is applied for N cycles at an initial $\Delta G=\Delta G_0$ value. The crack then propagates at the given ΔG_0 value and the crack growth rate can be determined. Once this first step is over, the ΔG value can be increased to $\Delta G_n=\Delta G_{n-1}+\Delta G_{increment}$, another set of N cycles is applied, another crack growth rate value is obtained and so on. This additional algorithm within the method was implemented within the software as shown in the flowchart in Figure 1. This flowchart shows both the method presented by Manca et al. in their paper (steps in blue) and the extra algorithm in order to run a test at multi-ΔG levels with one sample (in grey).

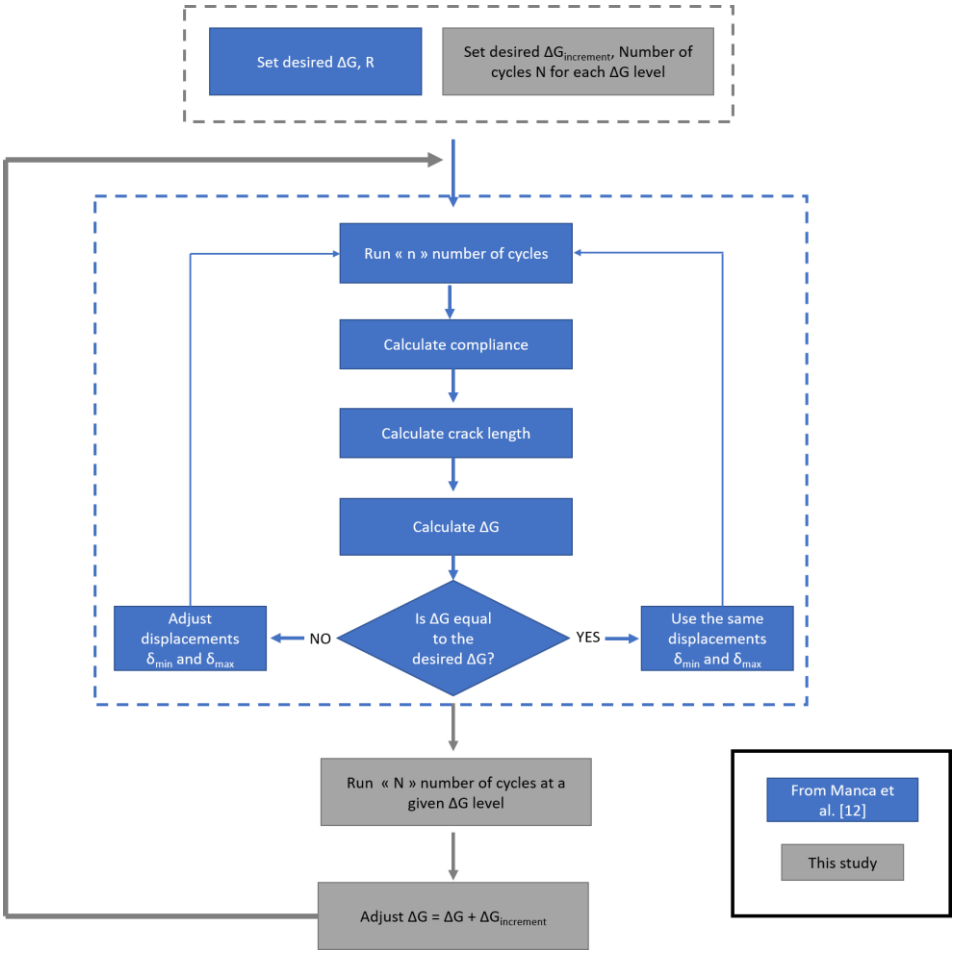

Figure 1: Flowchart of the multi-ΔG-control method

A total of 12 specimens were tested using the G-control method:

- 4 Specimens while running a multi-ΔG-control test, each using one specimen at 25 different ΔG levels

- 7 specimens while running a G-control test at various initial discrete ΔG_0 levels, in order to investigate whether the loading history affected crack propagation

3. Results

This part is divided in two main sections, devoted to static and fatigue tests results. Special emphasis is placed on the validation of the G-control method performed at different ΔG levels.

3.1. Static tests

Crack growth tests under static were performed first; R curves for the three specimens are shown in Figure 2.a. Associated results concerning critical strain energy release rate G_{Ic} are then presented in Figure 2.b. These were obtained using the compliance calibration (CC) method.

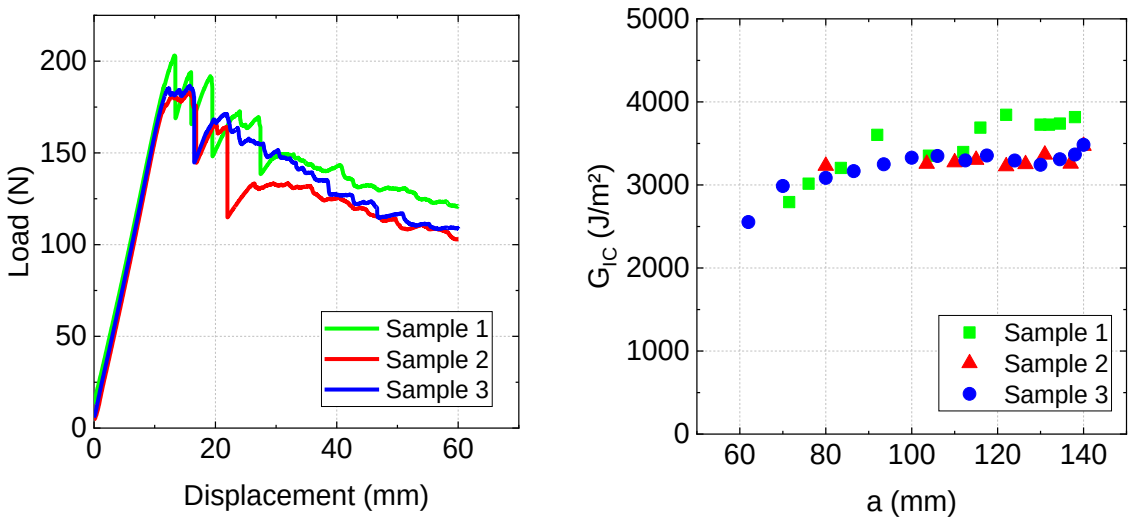

(a) (b)

Figure 2: Static DCB tests (a) Load-displacement plots (b) Fracture toughness as a function of crack length

Results from Figure 2.a show that the load-displacement plots exhibit an unstable behaviour at the start of propagation, as stick-slip is clearly identified up until 30 mm displacement. Stable propagation is then observed until the end of the test. As suggested by Davies et al. [31], when stick-slip is identified, propagation values can be divided in three types: first, unstable G_{IC} values corresponding to the onset of instability. Second, arrest values corresponding to the crack length after an unstable jump. Third, stable propagation values, here identified after 30 mm displacement. As a consequence, Figure 2.b shows fracture toughness values between 2000 and 4000 J/m². Results concerning each identified section are respectively 3180 ± 270 J/m² (Unstable), 2260 ± 300 J/m² (Arrest) and 3440 ± 280 J/m² (Stable). The latter exhibits the highest values. These results were obtained using the compliance calibration method. It may be noted that the modified beam theory (MBT) and modified compliance calibration (MCC) were also used, results are shown in Table 1 and show very little difference between the compliance calibration and the modified compliance calibration methods. Other methods are also found in literature [32].

Table 1: Stable critical strain energy release rate values calculated using the three methods suggested in ASTM D5528 [30]

Method	MBT	CC	MCC
G_{IC} (J/m²)	3628 ± 177	3440 ± 280	3466 ± 236

It may be noted that these values are also quite high compared to those of carbon/epoxy laminates or thermoset based composites in general [27], usually below 1000 J/m². Despite the fact that G_{IC} values for semi-crystalline thermoplastic composites are usually higher than those of thermosets, the stable propagation values found here (G_{IC} > 3000 J/m²) rank carbon/polyamide 6 in the upper range concerning fracture toughness in thermoplastic composites, Table 2.

Table 2: Critical strain energy release rate values from literature for thermoset and thermoplastic composites

Material	G_{IC} (J/m²)	Reference
Carbon/Epoxy (T300/5208)	100	Ramkumar & Whitcomb [33]
Carbon/Epoxy (AS4/3501-6)	250	Aliyu & Daniel [34]
Carbon/Epoxy (T300/934)	100	Garg & Ishai [35]
Carbon/Epoxy (T700/SR8100)	800	Le Guen-Geffroy et al. [36]
Glass/PP	2900	Davies & Cantwell [31]
Glass/PA66	1900	Davies & Moore [37]
Carbon/PPS	900	Chang & Lees [38]
Carbon/PEI	1200	Chang & Lees [38]
Carbon/PEEK	1600	Chang & Lees [38]
Carbon/PEEK (AS4/APC-1)	1400	Browning [39]
Carbon/PEEK (AS4/APC-2)	2900	Leach et al. [40]
Carbon/PEEK (AS4/APC-2)	1800	Gillepsie & Carlsson [41]
Carbon/PA	1100	Kinloch et al. [42]

3.2. Fatigue tests

The static fracture toughness value obtained in the previous section now serve as a reference for the fatigue tests, as it defines the range of strain energy release rate to investigate. The following sections are focused on fatigue tests. First, a subsection devoted to the validation of the G-control method is presented. Then, results from multi ΔG-control tests are shown.

3.2.1. Parameters entered in the multi ΔG-control method

Before testing, a certain number of parameters need to be fixed in the method. These are shown in Table 3.

Table 3: Input parameters in the multi ΔG-control method

ΔG_0 (J/m²)	$\Delta G_{increment}$ (J/m²)	$\Delta G_{tolerance}$ (J/m²)	R	Number of cycles per ΔG level	Frequency (Hz)
500	100	10	0.1	10 000	2

First, the initial ΔG_0 level was defined as 500 J/m². All tests were performed at an R-ratio ($\delta_{min}/\delta_{max}$) of 0.1. Based on equation 4, R_G is therefore equal to 0.01, meaning that G_{min} is very small compared to G_{max}. So ΔG is almost equal to G_{max}. Taking into account the G_{IC} value of 3440 ± 280 J/m², this indicates that the fatigue tests is started at around 15% of the static value. Coupled with a $\Delta G_{increment}$ of 100 J/m², this means that a wide range of ΔG levels can be studied. A total of 25 different ΔG levels were investigated for each specimen.

For each ΔG level, 10 000 cycles were applied. This number is arbitrary, but was chosen here so that the slope da/dN gave a correlation factor R^2 higher than 0.9 for all ΔG levels within this study. All specimens were pre-cracked before each fatigue test. However, it was necessary to perform 20 000 cycles at the first ΔG level to sharpen the crack tip. Indeed, the requirement of R^2=0.9 was only achieved when the first 10 000 cycles were excluded from the plot. This may be associated with fibre bridging, that was observed during the first 10 000 cycles. This is probably related to the fact that the insert used in our DCB specimens is slightly thicker than the ASTM 5528 [30] suggests, which may encourage an initial blunting effect.

3.2.2. Validation of the multi ΔG-control method

Concerning the validation of the methodology, as stated in section 2.3.2, two main conditions need to be fulfilled to make sure that the test is indeed performed at a constant and valid ΔG. First, it is necessary to show that the R-ratio is constant throughout the fatigue test. Second, the parameter δ_{max}/a^2 needs to be constant for a given ΔG, here ΔG=500 J/m² and ΔG=2900 J/m². Both of these conditions are supported by Figure 3.a and Figure 3.b.

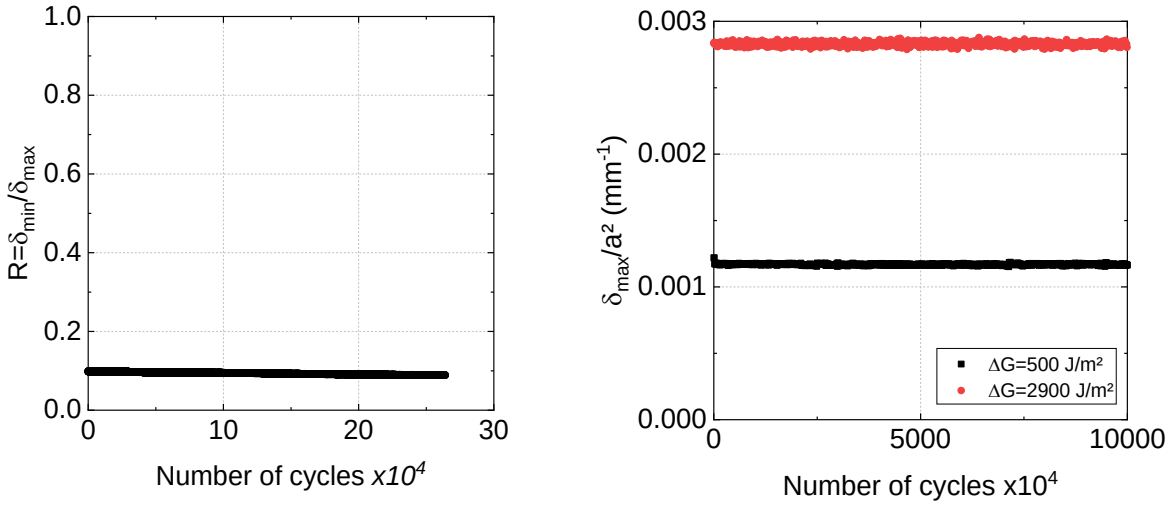

(a) (b)

Figure 3: (a) R-ratio as a function of number of cycles (b) δ_{max}/a^2 as a function of number of cycles for ΔG=500 J/m² and ΔG=2900 J/m²

Once these two conditions are fulfilled, we can plot ΔG as a function of the number of cycles, Figure 4.a, and this shows that the experimental ΔG value does indeed increase progressively throughout the test as programmed in the method. Additionally, we can show that the parameter δ_{max}/a^2 is constant for each ΔG level investigated here, Figure 4.b.

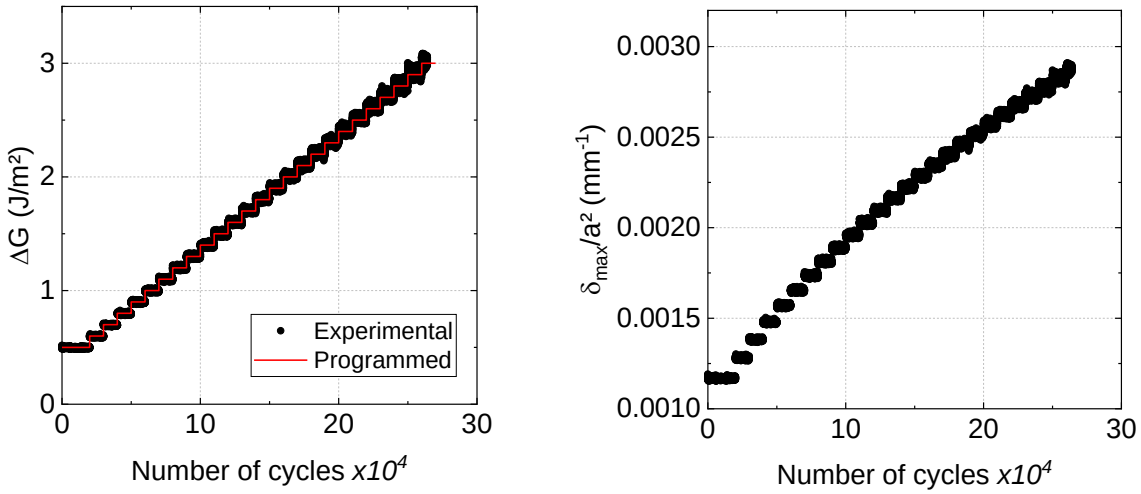

(a) (b)

Figure 4: (a) ΔG versus number of cycles (b) Constant δ_{max}/a^2 for each ΔG level investigated

A critical feature of the G-control method is the crack length calculation. Since it is based on compliance measurements, it needs to be verified. To do this, the Basler camera used in the static tests was used to record the crack length throughout one of the fatigue tests. Results from crack length measurements are compared to those of the crack length calculated from compliance measurements in Figure 5.

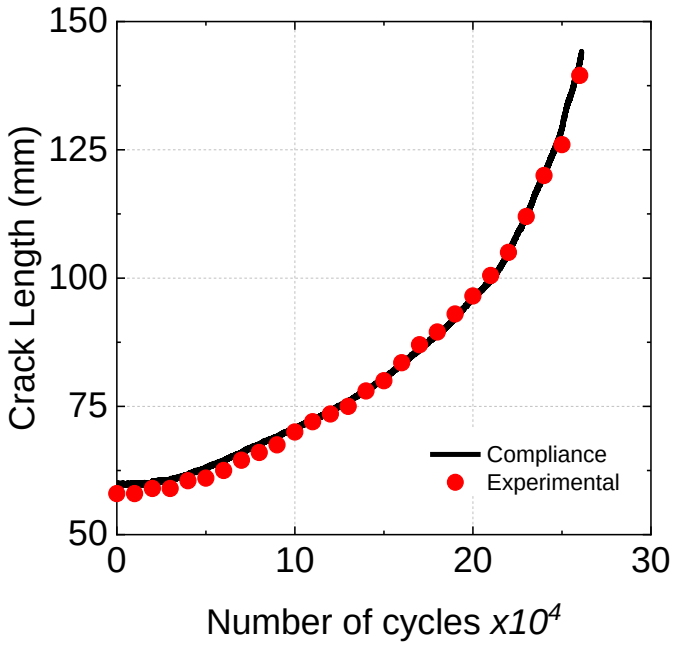

Figure 5: Crack length measured experimentally compared with crack length calculated from compliance measurements

From these results it is clear that the measured crack lengths are very close to those calculated using the compliance measurements. Slight differences can be observed, however, the crack length measurements are made through visual observation, which may be a source of error, especially at low ΔGs where crack propagation is very small. Nonetheless, this shows that the compliance measurements provide a good estimation of the crack length, so that it is possible to run cyclic crack growth tests at various ΔG levels.

3.2.3. Results from fatigue tests

Fatigue crack growth tests results are presented here. These tests were all performed at a frequency of 2 Hz and an R-ratio of 0.1, starting from ΔG_{min}=500 J/m² up to ΔG_{max}=2900 J/m². Every 10 000 cycles, the ΔG level was increased by $\Delta G_{increment}$=100 J/m², so 25 different strain energy release rate levels were applied within each

test and on each specimen. Figure 6 shows the change in crack length as a function of number of cycles for all the different ΔGs for one specimen.

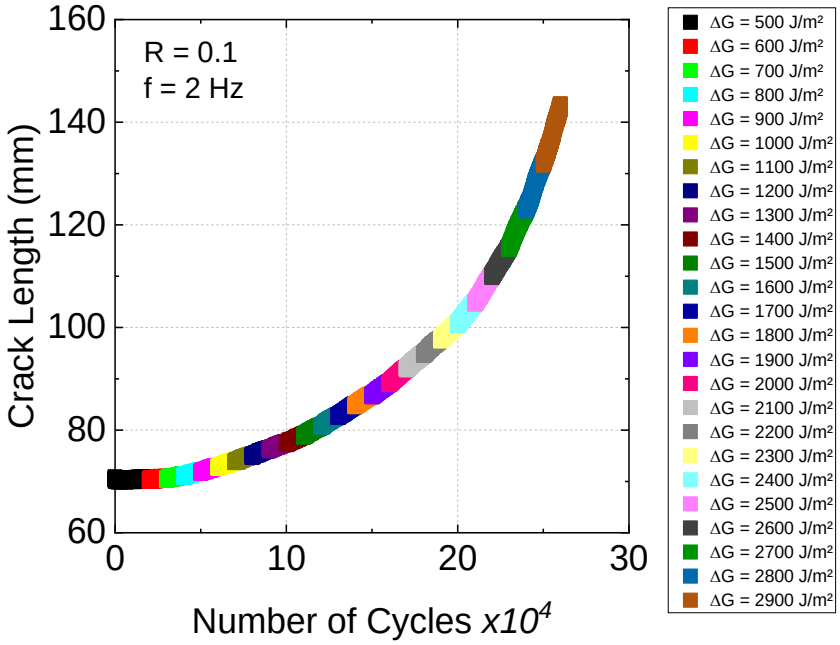

Figure 6: Crack length versus number of cycles for multiple ΔGs

Results from Figure 6 show that as the test proceeds, the crack growth rate (slope da/dN) evolves as ΔG increases. At low ΔGs (ΔG<~1000J/m²), the slope is quite flat, while at much higher ΔGs (ΔG>~2000 J/m²), the slope increases significantly. The crack growth rate obtained at each ΔG level is now plotted as a function of ΔG on a log-log scale for the four specimens tested, Figure 7.

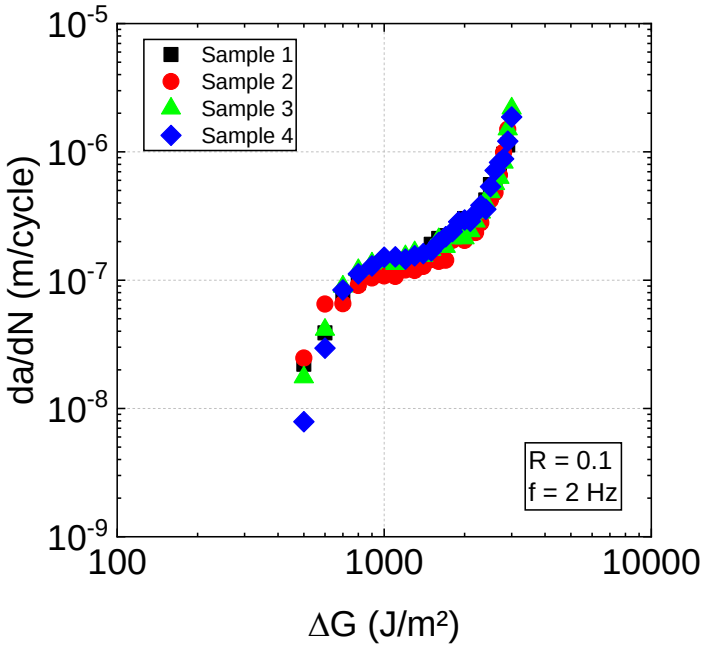

Figure 7: Crack growth rate as a function of ΔG

First, results in Figure 7 show little scatter. This is fairly surprising as results from literature may suggest otherwise. Two reasons may explain this result.

- First, low scatter may be associated with the G-control method in itself, in which the crack length is calculated from compliance. Figure 8 shows the difference between the crack growth rate calculated from compliance and the one measured experimentally (from Figure 5). Even if the overall tendency is similar, results show higher scatter when the crack growth rate is measured, more especially at the threshold region.

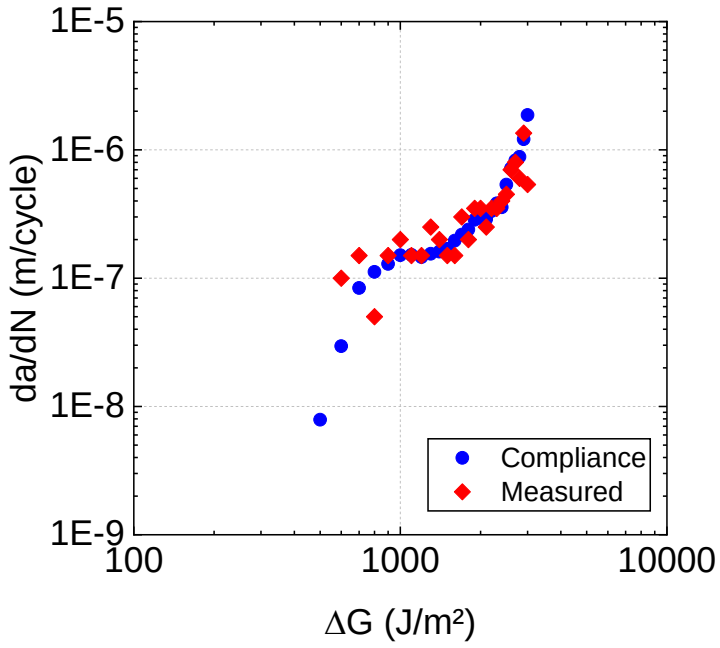

Figure 8 : Crack growth rate calculated from compliance and measured experimentally

- Second, the specimens used in this study are pure unidirectional specimens made with prepreg materials under carefully controlled conditions. Also, the prepreg does not contain weft fibres. Weft fibres are known to have an effect both on the static and fatigue results [43].

3.2.4. Influence of loading history

One of the potential limitations of this approach might be that damage introduced during cycling at one level affects the results when cycles are subsequently performed at a higher level. In order to establish whether crack propagation results were dependent on the previous loading history another series of tests was performed. New specimens were cycled at single ΔG_0 levels (7 specimens) for 20 000 cycles (the first 10 000 cycles were not taken into account to sharpen the crack tip) and results compared to those from multi-ΔG tests, Figure 9. It may be noted that such tests cycled at one single ΔG_0 level are similar to those from Manca et al. in [12]. Here, single tests were performed on a specimen at ΔG_0=700 J/m², ΔG_0=1000 J/m², ΔG_0=2300 J/m², ΔG_0=700 J/m² and finally 3 specimens were each tested at ΔG_0=1500 J/m². All other parameters were the same as previous tests described in section 3.2.3.

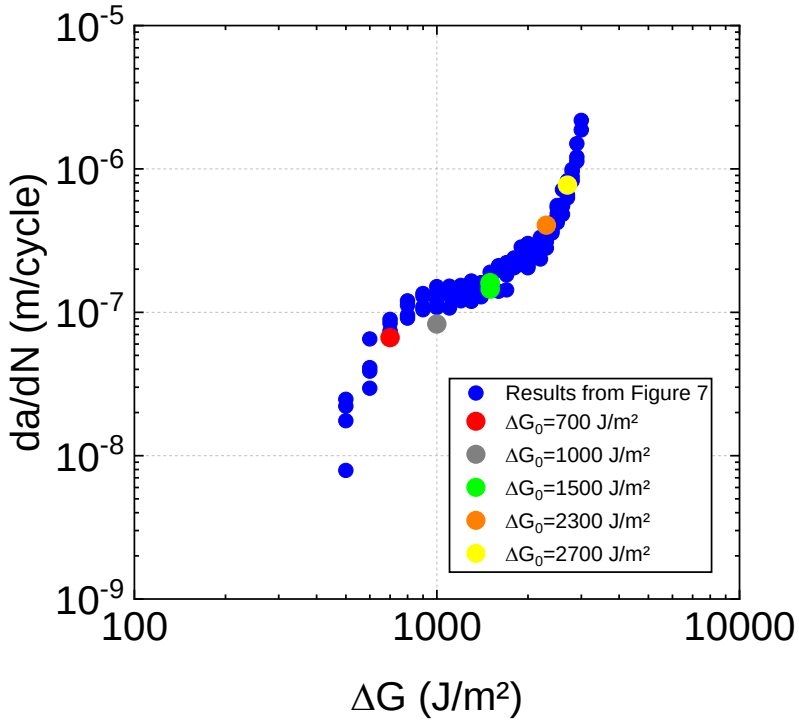

Figure 9: Multi ΔG tests vs tests performed at various ΔG_0 levels on multiple specimens

Figure 9 compares results from 4 multispecimen tests with those from the 7 single ΔG range tests. This indicates that new specimens cycled at different ΔG_0 levels give very similar crack growth rate results to those from multi ΔG tests. The only exception is the point at ΔG_0=1000 J/m² which is slightly lower than those from the multi-level tests, though this may simply be associated with experimental scatter. Figure 9 shows that the crack growth rate is independent of loading history. This demonstrates the strength of multi-ΔG tests, allowing a significant range of ΔG levels to be investigated with only one specimen.

4. Discussion

4.1. Identification of three different crack propagation regimes

According to the Paris law, there is a domain where the crack growth rate is considered log-linear with ΔG. However from Figure 7, the Paris law parameters cannot be determined directly, as all of three plots exhibit a sigmoidal shape. While it is common and known in literature to identify sigmoidal crack growth rates in metals, neat polymers and adhesives [24, 26, 44, 45], this is quite uncommon in composite materials. To the knowledge of the authors, very few data show such behaviour in long fibre reinforced composite materials with low scatter

[46-48]. The large ΔG range used in these tests (25 different ΔG levels) allows us to clearly identify three different crack propagation regimes, Figure 10.

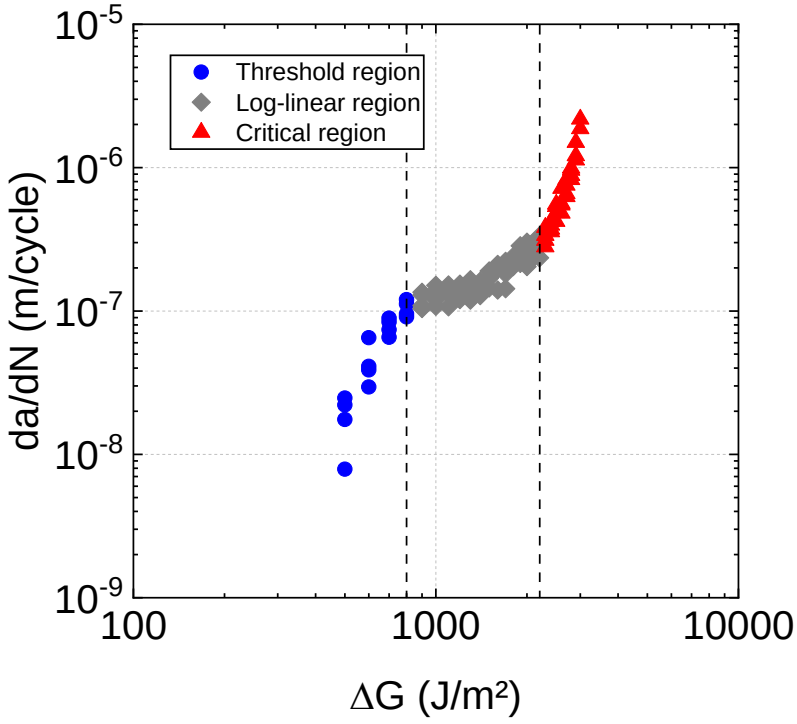

Figure 10: Identification of Paris law, $\Delta G_{threshold}$ and $\Delta G_{critical}$

In the first regime, the crack growth rate is extremely slow until it reaches a threshold value, here ΔG_{th}=900 J/m². In the second regime, the crack growth rate is log linear with ΔG and based on Equation 1, Paris law material parameters C and m can be identified as $1.03.10^{-10}$ m.cycle^{-1} and 1.02, respectively. The third regime is defined by a significant increase in the crack growth rate, here defined from ΔG_c=2200 J/m². ΔG_{th} and ΔG_c define the lower and upper bounds of the log-linear region. Surprisingly, the value of the exponent is quite low compared with results highlighted by Martin & Murri [20]. One possible reason is that exponents in thermoplastic composites tend to be lower than those of thermosets. This will be discussed in the next paragraph.

As stated in the introduction, published results from G-control tests are quite rare [6, 12]. Manca et al. [12] used the G-control method to characterize the fatigue crack growth behaviour of sandwich specimens under mixed mode loading, and therefore their results cannot be directly linked with the results shown in Figure 10. On the other hand, Russell & Street [6] did perform G-control tests under mode I loading on carbon/epoxy and carbon/PEEK specimens. From these tests, they were able to identify the Paris law parameters. These are shown in Table 4 and are compared to those identified from Figure 10. No published results on carbon/PA6 have been found for comparison.

Table 4: Paris law parameters from constant ΔG tests in this study and literature

Material	f (Hz)	R	C (m/cycle)	m	Reference
Carbon/PA6	2	0.1	$1.03.10^{-10}$	1.02	This study
Carbon/Epoxy	2.5	0.05	$2.1.10^{-24}$	9.4	Russell & Street [6]
Carbon/PEEK	1	0.05	$4.40.10^{-16}$	3	Russell & Street [6]

Usually, the most influent parameter on crack propagation in the Paris law is the exponent m. Here, it is clear that thermoplastic composites exhibit lower exponents, which result in lower crack propagation rates compared with their thermoset counterparts. Additionally, carbon/polyamide 6 has as an exponent close to 1, which suggests even slower crack propagation rates. To highlight such a statement, Figure 11 shows the crack propagation rates versus ΔG from this study and the results published by Russell & Street (within the ΔG bounds described in their paper).

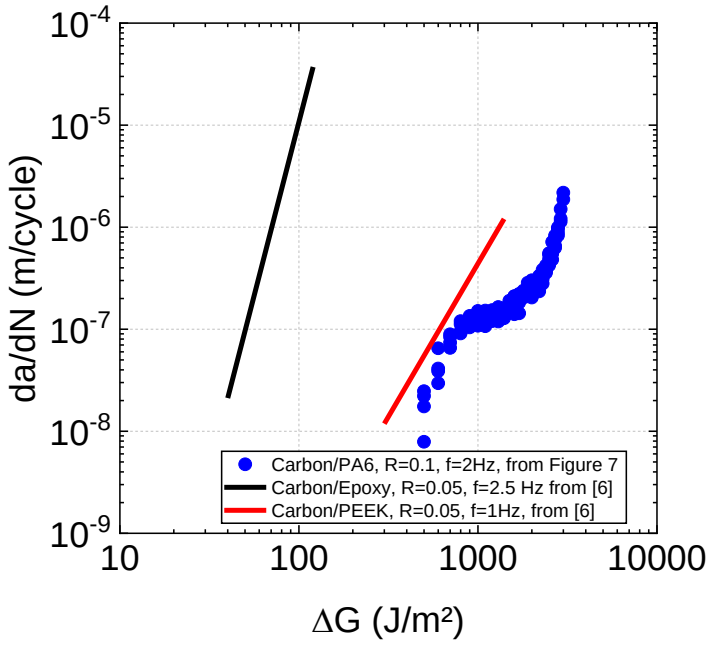

Figure 11: Data from Figure 7 vs data from Russell & Street [6] at constant ΔGs

To sum up, G-control tests revealed that the crack growth rate exhibited a sigmoidal behaviour as a function of ΔG. Within this sigmoidal behaviour, three different fatigue regimes were clearly identified. Lower and upper bounds ΔG_{th} and ΔG_c were determined as well as the fatigue parameters C and m. However, these

parameters cannot fully describe the sigmoidal behaviour observed here. The next section will focus on the description of the sigmoidal behaviour using the empirical Hartman-Shijves representation.

4.2. Application of the Hartman-Shijves equation to describe the experimental fatigue crack growth data

The empirical Hartman-Shijves representation has proved to be an interesting way to represent fatigue crack propagation in composites [23, 25]. It is applied here to try and describe the crack propagation behaviour of carbon/polyamide 6, in an attempt to fully describe the sigmoidal behaviour of Figure 7. However, some background on the Hartman Shijves equation will be presented first. It was initially developed to describe the fatigue crack growth data in metallic materials, Eq. 10 [26].

$$\frac{da}{dN} = D\left[\frac{\Delta K - \Delta K_{thr}}{1 - \sqrt{\frac{K_{max}}{A}}}\right]^n \quad \text{Eq.10}$$

Where D and n are material constants, ΔK_{thr} is associated with the threshold region and A a constant. For composite materials, fatigue crack growth tests usually involve the cyclic strain energy release rate ΔG and for similitude purposes, a modified Hartman-Shijves equation was defined, Eq.11.

$$\frac{da}{dN} = D\left[\frac{\Delta\sqrt{G} - \Delta\sqrt{G_{thr}}}{\sqrt{\left[1 - \sqrt{\frac{G_{max}}{A}}\right]}}\right]^n \quad \text{Eq.11}$$

Where $\Delta\sqrt{G}$ is the range of the applied strain energy release rate, $\Delta\sqrt{G_{thr}}$ the range of the fatigue threshold value of $\Delta\sqrt{G}$. First, it should be remembered that the Hartman-Shijves representation takes into account $\Delta\sqrt{G}$ instead of ΔG, so results from Figure 8 cannot be directly transposed here. $\Delta\sqrt{G}$ is defined as follows, Eq. 12.

$$\Delta\sqrt{G} = \sqrt{G_{max}} - \sqrt{G_{min}} \quad \text{Eq.12}$$

An important feature of the Hartman-Shijves representation is the determination of $\Delta\sqrt{G_{thr}}$. It is defined in Eq. 13.

$$\Delta\sqrt{G_{thr}} = \sqrt{G_{thr\,max}} - \sqrt{G_{thr\,min}} \quad \text{Eq.14}$$

Based on our results, $\Delta\sqrt{G_{thr}}$ is found equal to 20 $J^{1/2}/m$. The determination of the constant A is also essential. As stated by Jones et al. [24], A is associated with the third, rapid crack propagation regime. In our case, A was taken as 2900 J/m^2, i.e. the last ΔG level, at which the crack propagated at a high rate. All the parameters needed in the

Hartman-Shijves representation are now obtained. Finally, da/dN is plotted as a function of $\frac{\Delta\sqrt{G}-\Delta\sqrt{G_{thr}}}{\sqrt{\left[1-\sqrt{\frac{G_{max}}{A}}\right]}}$ in Figure 12.

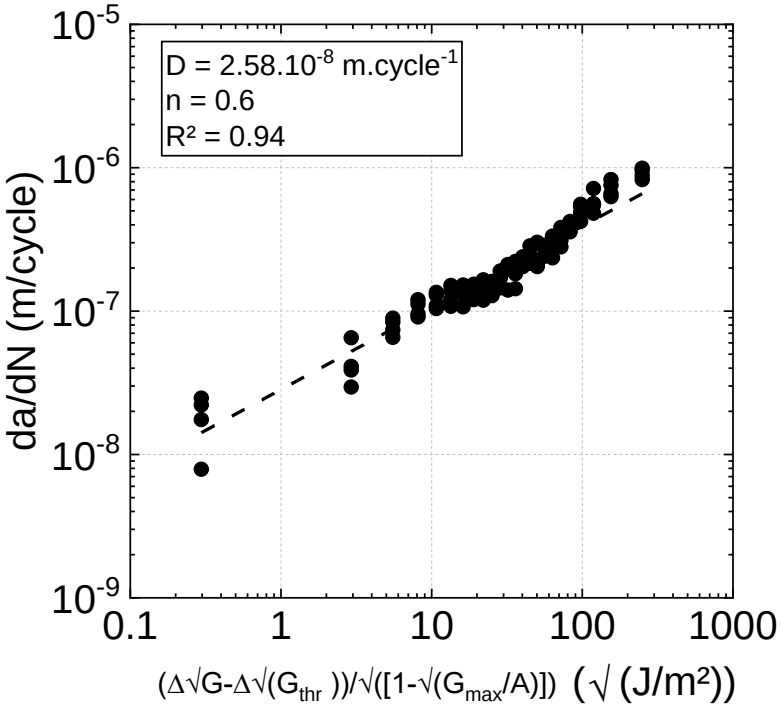

Figure 12: Hartman-Shijves representation of data in Figure 7

First, results show that a log-linear relationship is obtained with a good correlation factor (0.94). Second, such a master curve allows us to determine the parameters D and n from Eq.11. These are respectively equal to $2.58.10^{-8}$ m.cycle^{-1} and 0.6. The parameters used for the Hartman-Shijves representation are now summarized in Table 5. It may be noted that these parameters were used for all 4 samples considered here.

In the published literature, the exponent m in the Paris law is usually relatively large for composite materials (m>5) [20, 49]. Working with large n values leads to high uncertainties in the crack growth rate prediction. The Hartman-Shijves somewhat diminishes the value of the exponent n and therefore allows for lower errors in calculation. This was confirmed here, as the exponent for Hartman-Shijves (n=0.6) is lower than that of the Paris law (m=1.02). However, it was shown earlier that the value of m for C/PA6 was already quite low. So the main interest of the Hartman-Shijves representation resides here in the description of the crack growth behaviour from slow to fast crack propagation rates, rather than lowering the value of the exponent.

Table 5: Parameters for the Hartman-Shijves representation

D (m.cycle^{-1})	n	A (J/m^2)	ΔG_{thr} (J/m^2)
$2.58.10^{-8}$	0.6	2900	20

These parameters can now be used to try and describe the sigmoidal behaviour observed earlier; results are presented in Figure 13.

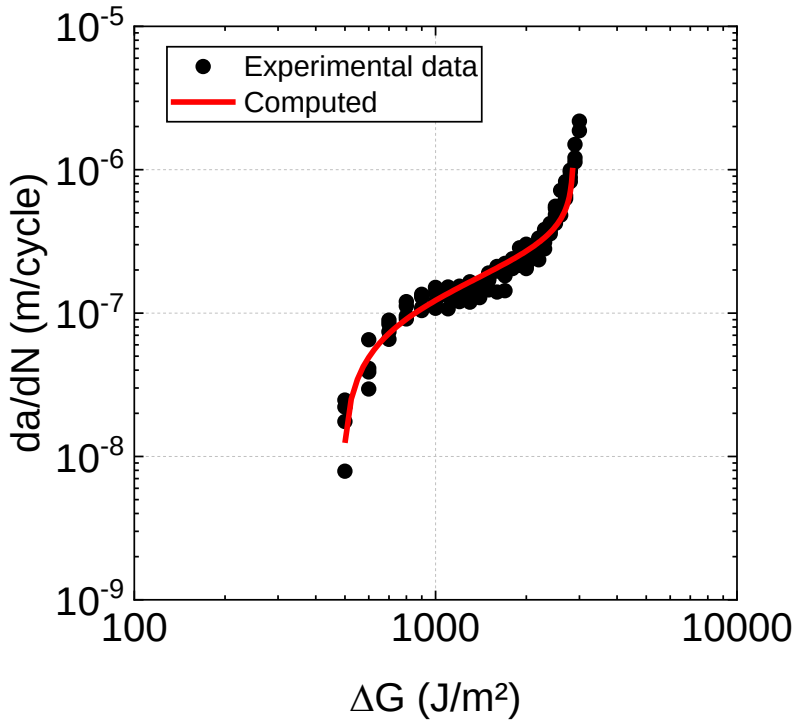

Figure 13: Experimental data compared with computed Hartman-Shijves description

Using the parameters given in Table 5 in the Hartman-Shijves equation, it is clear that the experimental data can be described quite accurately. A reasonable description is obtained from slow to fast crack propagation rates and this provides a powerful descriptive tool compared with the simpler representation based on the Paris law.

4.3. Multi-ΔG control test - A means to perform fast and reliable fatigue crack growth tests

Through the results presented in this paper, the multi ΔG control test method has been shown to provide a powerful tool to investigate the fatigue crack growth behaviour of composites. Additionally, an aspect that has not been discussed yet is the fact that such a method, when optimized, can lead to significantly shorter fatigue crack growth tests. Manca et al. [12] demonstrated that it was possible to obtain three different propagation rate

values associated with a given ΔG level within one hour of testing. This allowed them to identify Paris law parameters very quickly. In the present study, using three ΔG levels corresponds to approximately 5 hours of testing to obtain the Paris law parameters. However, here the multi-ΔG test on one specimen lasted for about 250 000 cycles, so about 35 hours at 2 Hz. This duration allowed for the identification of the complete crack propagation curve with 25 ΔG levels, providing the three crack propagation regimes (threshold, log linear and catastrophic) through the validation Hartman-Shijves equation. In our opinion, this represents a significant benefit compared to methods that do not include G-control tests, especially considering that G-control tests in both Manca's work and our study were performed at relatively low frequencies (1 and 2 Hz respectively). (This frequency was selected here after a preliminary study with IR camera measurements indicated no heating at this temperature). However, in [15], Wilk describes a compliance based test which allows for the determination of Paris law parameters with good accuracy within 56 hours at 10 Hz and in [14] Brunner et al. obtained the Paris law parameters within 8 to 24 hours of testing at 10 Hz. This means that by increasing the frequency, provided heating does not occur multi ΔG-control tests could provide Paris law parameters as well as Hartman-Shijves parameters within a day of testing.

5. Conclusion

The mode I fatigue crack properties were studied through the use of a multi-ΔG-control method, i.e. a test performed at several constant ΔG levels on one specimen. The latter was successfully implemented within the electric test machine software. A total of 25 different ΔG levels were programmed consecutively, which allowed the study of the crack growth behaviour of carbon/polyamide 6 unidirectional composites. Results highlighted a crack growth behaviour in the form of a sigmoid rather than a simple log-linear plot. This result demonstrated the limits of the more traditional Paris law representation for crack growth rate. An alternative approach, based on the Hartman-Shijves equation, was then used to more accurately describe the sigmoidal crack growth behaviour obtained from the multi-ΔG-control tests. This work has shown that the multi-ΔG control method can provide reliable crack growth propagation results.

Future work includes several aspects. First, the results presented in this work were obtained while increasing the ΔG level every 10 000 cycles. It would be interesting to investigate whether the same results are obtained when decreasing ΔG throughout the test, on the same C/PA6 material used here but also on more traditional composite materials such as C/Epoxy and C/PEEK. This would help to clarify to what extent these curves represent intrinsic material properties. Second, the work carried out in this paper is part of a project focused on the repair of

thermoplastic composites after use for several years in the marine environment. The results show exceptional crack growth resistance for these polyamide based composites in the dry condition, but these materials are also sensitive to moisture. It will be interesting to evaluate changes in the parameters within the Hartman-Shijves equation after both aging and repair.

Acknowledgments

The authors would like to thank the scientific direction of Ifremer for the funding of the REPACOMP project.

References

[1] Harris, B. (Ed.). (2003). Fatigue in composites: science and technology of the fatigue response of fibre-reinforced plastics. Woodhead Publishing.

[2] Talreja, R., & Varna, J. (Eds.). (2015). Modeling damage, fatigue and failure of composite materials. Elsevier.

[3] Hojo, M., Matsuda, S., Fiedler, B., Kawada, T., Moriya, K., Ochiai, S., & Aoyama, H. (2002). Mode I and II delamination fatigue crack growth behavior of alumina fiber/epoxy laminates in liquid nitrogen. *International Journal of Fatigue*, 24(2-4), 109-118.

[4] Hojo, M., Ando, T., Tanaka, M., Adachi, T., Ochiai, S., & Endo, Y. (2006). Modes I and II interlaminar fracture toughness and fatigue delamination of CF/epoxy laminates with self-same epoxy interleaf. *International Journal of Fatigu*e, 28(10), 1154-1165.

[5] Ewald HL, , Wanhill RJH. Fracture mechanics, (1984), Butterworth-Heinemann. London.

[6] Russell, A. J., & Street, K. N. (1988, January). A constant ΔG test for measuring mode I interlaminar fatigue crack growth rates. In Composite Materials: Testing and Design (Eighth Conference). ASTM International.

[7] Tanaka, K., Tanaka, H., Tsuji, T., & Yamagishi, K. (1995). Effect of stress ratio on mode I propagation of interlaminar fatigue cracks in CFRP. *Zairyo*, *44*(502), 960-966.

[8] Hojo, M., Ochiai, S., Aoki, T., & Ito, H. (1995). Mode I fatigue delamination for CF/PEEK laminates using maximum-energy-release-rate constant tests. *Zairyo*, *44*(502), 953-959.

[9] Hojo, M., Ochiai, S., Aoki, T., & Ito, H. (1995). Measurement of delamination fatigue threshold and its crack-length dependency for CF/PEEK laminates. *Trans. Jpn. Soc. Mech. Eng.,(in Japanese)*, *61*(583), 516-522.

[10] Sato, N., Hojo, M., & Nishikawa, M. (2015). Intralaminar fatigue crack growth properties of conventional and interlayer toughened CFRP laminate under mode I loading. *Composites Part A: Applied Science and Manufacturing*, *68*, 202-211.

[11] Hojo, M., Ochiai, S., Aoki, T., & Ito, H. (1994). New simple and practical test method for interlaminar fatigue threshold in CFRP laminates. In *Proceedings 2nd Conference on Composites Testing and Standardisation (Hogg PJ, Schulte K. Wittich H., eds.)* (pp. 553-561).

[12] Manca, M., Berggreen, C., & Carlsson, L. A. (2015). G-control fatigue testing for cyclic crack propagation in composite structures. *Engineering Fracture Mechanics*, 149, 375-386.

[13] Murri, G. B. (2014). Effect of data reduction and fiber-bridging on Mode I delamination characterization of unidirectional composites. *Journal of Composite Materials*, *48*(19), 2413-2424.

[14] Brunner, A. J., Murphy, N., & Pinter, G. (2009). Development of a standardized procedure for the characterization of interlaminar delamination propagation in advanced composites under fatigue mode I loading conditions. *Engineering Fracture Mechanics*, 76(18), 2678-2689.

[15] Wilk, J. (2018). Compliance based method for testing fatigue delamination propagation in laminates. *Engineering Fracture Mechanics*, 203, 137-151.

[16] Masaki, H., Shojiro, O., Gustafson, C. G., & Keisuke, T. (1994). Effect of matrix resin on delamination fatigue crack growth in CFRP laminates. *Engineering Fracture Mechanics*, *49*(1), 35-47.

[17] Hojo, M., Gustafson, C. G., Tanaka, K., & Hayashi, R. (1987). Mode I propagation of delamination fatigue cracks in CFRP. In *Advanced Materials for Severe Service Applications* (pp. 353-372). Springer, Dordrecht.

[18] Hojo, M., Tanaka, K., Gustafson, C. G., & Hayashi, R. (1987). Effect of stress ratio on near-threshold propagation of delimination fatigue cracks in unidirectional CFRP. *Composites Science and Technology*, *29*(4), 273-292.

[19] Paris, P. C. Gomez, AP, Anderson WE, (1961). A rational analytic theory of fatigue. The trend of engineering, 13, 9-14.

[20] Martin, R. H., & Murri, G. B. (1990). Characterization of mode I and mode II delamination growth and thresholds in AS4/PEEK composites. In Composite materials: testing and design (Ninth Volume). ASTM International.

[21] Pascoe, J. A., Alderliesten, R. C., & Benedictus, R. (2013). Methods for the prediction of fatigue delamination growth in composites and adhesive bonds–a critical review. *Engineering Fracture Mechanics*, 112, 72-96.

[22] Khan, R., Alderliesten, R., Badshah, S., & Benedictus, R. (2015). Effect of stress ratio or mean stress on fatigue delamination growth in composites: critical review. *Composite Structures*, 124, 214-227.

[23] Jones, R., Pitt, S., Brunner, A. J., & Hui, D. (2012). Application of the Hartman–Schijve equation to represent Mode I and Mode II fatigue delamination growth in composites. *Composite Structures*, 94(4), 1343-1351.

[24] Jones, R., Hu, W., & Kinloch, A. J. (2015). A convenient way to represent fatigue crack growth in structural adhesives. *Fatigue & Fracture of Engineering Materials & Structures*, 38(4), 379-391.

[25] Jones, R., Kinloch, A. J., & Hu, W. (2016). Cyclic-fatigue crack growth in composite and adhesively-bonded structures: The FAA slow crack growth approach to certification and the problem of similitude. *International Journal of Fatigue*, 88, 10-18.

[26] Hartman, A., & Schijve, J. (1970). The effects of environment and load frequency on the crack propagation law for macro fatigue crack growth in aluminium alloys. *Engineering Fracture Mechanics*, 1(4), 615-631.

[27] Sela, N., & Ishai, O. (1989). Interlaminar fracture toughness and toughening of laminated composite materials: a review. *Composites*, 20(5), 423-435.

[28] Pemberton, R., Summerscales, J., & Graham-Jones, J. (Eds.). (2018). *Marine composites: design and performance*. Woodhead Publishing.

[29] Arhant, M., Le Gac, P. Y., Le Gall, M., Burtin, C., Briançon, C., & Davies, P. (2016). Effect of sea water and humidity on the tensile and compressive properties of carbon-polyamide 6 laminates. *Composites Part A:* 91, 250-261.

[30] AC09036782, A. (Ed.). (2007). *Standard test method for mode I interlaminar fracture toughness of unidirectional fiber-reinforced polymer matrix composites*. ASTM Internat.

[31] Davies, P., & Moore, D. R. (1990). Glass/Nylon-6.6 composites: delamination resistance testing. *Composites Science and Technology*, 38(3), 211-227.

[32] Kageyama, K., Kobayashi, T., & Chou, T. W. (1987). Analytical compliance method for Mode I interlaminar fracture toughness testing of composites. *Composites*, *18*(5), 393-399.

[33] Ramkumar, R. L., & Whitcomb, J. D. (1985). Characterization of mode I and mixed-mode delamination growth in T300/5208 graphite/epoxy. In Delamination and debonding of materials. ASTM International.

[34] Aliyu, A. A., & Daniel, I. M. (1985). Effects of strain rate on delamination fracture toughness of graphite/epoxy. In Delamination and debonding of materials. ASTM International.

[35] Garg, A., & Ishai, O. (1985). Hygrothermal influence on delamination behavior of graphite/epoxy laminates. *Engineering Fracture Mechanics*, 22(3), 413-427.

[36] Le Guen-Geffroy, A.; Davies, P.; Le Gac, P.-Y.; Habert, B. (2020), Influence of Seawater Ageing on Fracture of Carbon Fiber Reinforced Epoxy Composites for Ocean Engineering. *Oceans*, 1, 198-214.

[37] Davies, P., & Cantwell, W. J. (1994). Fracture of glass/polypropylene laminates: influence of cooling rate after moulding. *Composites*, 25(9), 869-877.

[38] Chang, I. Y., & Lees, J. K. (1988). Recent development in thermoplastic composites: a review of matrix systems and processing methods. Journal of thermoplastic composite materials, 1(3), 277-296.

[39] Browning, C. E. (1984). Composite Materials Characterization and Development at AFWAL. Tough Composite Materials, NASA Conference Publication 2334 , 33.

[40] Leach, D. C., Curtis, D. C., & Tamblin, D. R. (1985). Delamination behaviour of aromatic polymer composite APC-2'. In ASTM Symp on Toughened Composites, Houston, TX.

[41] Gillespie Jr, J. W., Carlsson, L. A., & Smiley, A. J. (1987). Rate-dependent mode I interlaminar crack growth mechanisms in graphite/epoxy and graphite/PEEK. Composites Science and Technology, 28(1), 1-15.

[42] Kinloch, A. J., Kodokian, G. K. A., & Watts, J. F. (1992). The adhesion of thermoplastic fibre composites. Philosophical Transactions of the Royal Society of London. Series A: Physical and Engineering Sciences, 338(1649), 83-112.

[43] Alif, N., Carlsson, L. A., & Boogh, L. (1998). The effect of weave pattern and crack propagation direction on mode I delamination resistance of woven glass and carbon composites. *Composites Part B: Engineering*, *29*(5), 603-611.

[44] Cano, A. J., Salazar, A., & Rodríguez, J. (2018). Evaluation of different crack driving forces for describing the fatigue crack growth behaviour of PET-G. *International Journal of Fatigue*, *107*, 27-32.

[45] Chaffin, K. A., Wilson, C. L., Himes, A. K., Dawson, J. W., Haddad, T. D., Buckalew, A. J., ... & Simha, N. K. (2013). Abrasion and fatigue resistance of PDMS containing multiblock polyurethanes after accelerated water exposure at elevated temperature. *Biomaterials*, *34*(33), 8030-8041.

[46] Shivakumar, K., Chen, H., Abali, F., Le, D., & Davis, C. (2006). A total fatigue life model for mode I delaminated composite laminates. *International Journal of Fatigue*, *28*(1), 33-42.

[47] Brunner, A. J., Stelzer, S., Pinter, G., & Terrasi, G. P. (2016). Cyclic fatigue delamination of carbon fiber-reinforced polymer-matrix composites: Data analysis and design considerations. *International Journal of Fatigue*, *83*, 293-299.

[48] Christopoulos, G. C., & Paipetis, S. A. (1993). Interlaminar Fatigue Crack Propagation in Mode I of Carbon Fiber/PEEK Composites. *Advanced Composites Letters*, *2*(1), 096369359300200101.

[49] Zhu, M., Gorbatikh, L., Fonteyn, S., Van Hemelrijck, D., Pyl, L., Carrella-Payan, D., & Lomov, S. V. (2020). Digital image correlation assisted characterization of Mode I fatigue delamination in composites. *Composite Structures*, 253, 112746.